Characterization of the Copper- and Silver–Thiolate Clusters in N-Terminal Fragments of the Yeast ACE1 Transcription Factor Capable of Binding to Its Specific DNA Recognition Sequence†

José R. Casas-Finet,‡ Stella Hu,§ Dean Hamer,§ and Richard L. Karpel*,‡

Department of Chemistry and Biochemistry, University of Maryland Baltimore County, Baltimore, Maryland 21228, and Laboratory of Biochemistry, National Cancer Institute, National Institutes of Health, Bethesda, Maryland 20892

Received December 3, 1991; Revised Manuscript Received April 28, 1992

ABSTRACT: N-terminal fragments of ACE1 protein spanning residues 1–122 or 1–110, termed ACE1(122*) and ACE1(110*), respectively, were investigated in regard to their metal- and double-stranded DNA-binding properties. Band mobility shift assays showed that binding to a specific oligonucleotide (termed UASc), containing two ACE1(122*) binding sites, requires the presence of Cu(I) or Ag(I) but does not occur in the presence of divalent metal ions. Both the Ag(I) and the Cu(I) forms of ACE1(122*) were characterized spectroscopically. The Tyr and metal cluster luminescence emission of Cu–ACE1(122*) was specifically quenched by the oligonucleotide UAScL, but not by an oligonucleotide of the same length and base composition but scrambled sequence. The room-temperature luminescence of Cu(I)–ACE1(122*) was assigned to a phosphorescence emission, on the basis of its long-lived luminescence of ~3.5 μs. We report the first observation of a Ag(I) metal cluster in solution for Ag(I)–ACE1(122*), which was found to exhibit a quantum yield and average luminescence lifetime that are ca. 6% of that of Cu(I)–ACE1(122*). The three-dimensional structure brought about by the binding of either metal ion appears to be very similar, since dynamic tyrosine fluorescence lifetime measurements, as well as circular dichroism spectra, were nearly identical for Cu– and Ag–ACE1(122*). Based on these results, we present a hypothetical model for the structure of the metal cluster in this class of proteins.

The ACE1 protein (also known as CUP2) of *Saccharomyces cerevisiae* is a regulatory gene product involved in the control of the transcription of CUP1, the yeast metallothionein gene, in the presence of Cu (Thiele, 1988) and Ag ions (Fürst et al., 1988). Among its 225 amino acid residues, ACE1 contains 12 Cys and an excess of basic residues located in an amino-terminal region (residues 1–122) which is involved in the metal-dependent binding to the specific upstream activation sequences (UAS) (Fürst et al., 1988). The active form of ACE1 has been proposed to contain a Cu(I)–cysteinyl thiolate polynuclear cluster that induces a conformational alteration required for DNA binding to its specific activator sequence (Fürst et al., 1988).

In our initial report on the spectroscopic properties of the Cu(I)-bound N-terminal ACE1 fragment spanning residues 1–122, ACE1(122*) (Casas-Finet et al., 1991), we demonstrated the existence of charge-transfer and/or metal-centered ultraviolet absorption bands, as well as the emission by the sample of room-temperature orange luminescence characteristic of Cu(I)–S clusters. Observation of these properties was dependent on the binding of the metal in the +1 oxidation state, since addition of Cu(I)-, but not Cu(II)-chelating agents abolished the effects. Using intrinsic Tyr static fluorescence or the metal cluster luminescence, we monitored binding of Cu(I)–ACE1(122*) to a 22-bp oligonucleotide (UAScL) containing the leftward half of its specific DNA recognition site.

In this work, we have extended our earlier investigation of the metal- and DNA-binding domain of ACE1 protein to characterize the Ag(I) and the Cu(I) forms of the domain. We show via electrophoretic band mobility shift assays that binding to a specific double-stranded oligonucleotide (termed UASc), containing two ACE1(122*) binding sites, requires the presence of monovalent metal ions. As observed previously for Cu(I), Ag(I) uptake leads to a form of ACE1(122*) capable of binding UASc. The room-temperature luminescence spectra of Ag(I)–ACE1(122*) and the luminescence lifetimes of Cu(I)–ACE1(122*) and Ag(I)–ACE1(122*) were measured. To our knowledge, this is the first report of ambient temperature luminescence for a Ag(I) metal cluster in solution. The luminescence emission of Ag–ACE1(122*) does not seem to originate from a small amount of contaminating Cu–ACE1(122*), as both the wavelength of maximum emission and the luminescence lifetime components differ from those of Cu–ACE1(122*). Moreover, the luminescence excitation spectrum λ_{max} coincides with the wavelength of maximum absorbance for the metal cluster of Ag–ACE1(122*), but not Cu–ACE1(122*). The Tyr fluorescence emission of Ag–ACE1(122*) was specifically quenched by the oligonucleotide UAScL, but not by an oligonucleotide of the same length and base composition but scrambled sequence. We have also studied a shorter fragment of the ACE1 protein that spans residues 1–110, ACE1(110*), and show that the Cu–ACE1-(110*) peptide exhibits luminescence properties practically indistinguishable from those of the longer peptide and is active in specific UAScL binding. Our results, taken together with other recent studies on ACE1 and related systems (Dameron et al., 1991), allow us to present a hypothetical model for the structure of the metal cluster in the N-terminal DNA-binding domain of ACE1 protein.

Materials and Methods

An *Escherichia coli* phage T7 overexpression system was used to overproduce a polypeptide containing the amino-terminal 122 or 110 amino acids of the ACE1 protein, together

† This work was supported by a grant from the American Cancer Society, NP-671 (to R.L.K.).

‡ University of Maryland.

§ National Cancer Institute.

0006-2960/92/0431-6617$03.00/0

with 19 residues from the vector (Casas-Finet et al., 1991). ACE1(122*) and ACE1(110*) were purified as previously described (Casas-Finet et al., 1991) and were >98% pure as assayed by Coomassie Brilliant Blue-stained 15% SDS–polyacrylamide gel electrophoresis (note that ACE1 migrates abnormally slowly on SDS gels). Either polypeptide appeared as a single peak in elution profiles of reverse-phase HPLC on a Waters C_{18} μ-Bondapak column, performed as previously described (Casas-Finet et al., 1992). Protein concentration was determined by amino acid analysis on a Beckman 6300 instrument, which revealed a composition identical to that predicted from the nucleotide sequence. N-Terminal sequencing was carried out by automated Edman degradation on an Applied Biosystems 475 sequencer and yielded the expected sequence for the first 10 residues of ACE1(122*). Metal content was determined by flame atomic absorption spectroscopy on a Perkin-Elmer 305A instrument. The Cu–ACE1(122*) and Cu–ACE1(110*) samples used for this work contained molar Cu to polypeptide ratios of 6.8 ± 0.2 and 7.1 ± 0.2, respectively.

Ag–ACE1(122*) was purified from *E. coli* carrying the T7-ACE1(122*) expression plasmid. Cells were grown and induced with isopropyl β-D-thiogalactopyranoside (IPTG) as described previously (Casas-Finet et al., 1991) except that $CuSO_4$ was omitted from the growth medium. A crude extract was prepared according to published procedures (Casas-Finet et al., 1991); $AgNO_3$ was then added to aliquots of the clarified extract and incubated at room temperature for 10 min. The aliquots were heat-treated (70 °C for 7 min) and centrifuged at 12000*g* for 15 min. A portion of the supernatant was tested in a band mobility shift assay using ^{32}P-labeled UASc oligonucleotide (see below). Maximum activity was reconstituted at 300 μM $AgNO_3$. The rest of the crude extract was reconstituted with 300 μM $AgNO_3$, and Ag–ACE1(122*) was purified by following a protocol identical to that used for the Cu(I) complex. The metal stoichiometry of Ag–ACE1(122*) was 7.3 ± 0.2 mol of Ag/mol of peptide.

Cu–ACE1(122*), Ag–ACE1(122*), and Cu–ACE1(110*) samples were kept under N_2 at −70 °C in sealed containers until used. Protein samples were prepared in either 10 mM sodium cacodylate or 10 mM sodium phosphate, pH 6.15, previously degassed and saturated with dry nitrogen; sample handling was carried out in a glovebag under nitrogen atmosphere. KCl (reagent grade), sodium cacodylate, sodium phosphate (monobasic), and sodium phosphate (dibasic) were from Sigma. $CuSO_4$, CuCl, $AgNO_3$, KCN, disodium ethylenediaminetetraacetic acid (Na_2EDTA), and sodium diethyldithiocarbamate (DDC) were purchased from Aldrich and dissolved in Millipore-filtered H_2O with a conductivity of 18 mΩ^{-1}. Cu(I)–acetonitrile was prepared by the method of Hemmerich and Sigwart (1963).

The 42-bp UASc oligonucleotide containing residues 145–103 of the *CUP1* gene (5′-GATGCGTCTTTTCCGCTGAACCGTTCCAGCAAAAAAGACTAG-3′) contains two binding sites for ACE1. Three shorter, overlapping oligonucleotides containing the left (L), middle (M), and right (R) sequences of UASc were annealed to their complementary sequences to form the double-stranded species: UAScL (5′-GATGCGTCTTTTCCGCTGAACC-3′), UAScM (5′-GTCTTTTCCGCTGAACCGTTCCAG-3′), and UAScR (5′-GTTCCAGCAAAAAAGACTAG-3′). MixL (5′-CTGAATGTTCGTGAGCTCTCCC-3′), an oligonucleotide of base composition identical to that of UAScL but with scrambled sequence, was annealed to its complementary sequence and the double-stranded species was used as a control in binding studies. Oligonucleotides were synthesized on an Applied Biosystems apparatus and purified by denaturing gel electrophoresis. Complementary oligonucleotides were separately labeled with polynucleotide kinase and [γ-^{32}P]ATP, mixed, boiled, and annealed for 15 min. The double-stranded form was then purified by electrophoresis through a native 12% polyacrylamide gel.

Electrophoretic band mobility shift assays were performed using 10 fmol of ^{32}P-labeled oligonucleotides (5.0×10^4 cpm); samples (20 μL) were loaded onto a 4% polyacrylamide gel in 25 mM Tris–borate buffer, pH 8.3, containing 2.5 mM EDTA, and run for 2–3 h at a constant current of 25 mA. The gel was fixed, dried, and autoradiographed for 1–2 h.

Absorption spectra were acquired at 25.0 ± 0.1 °C on a Gilford Response spectrophotometer using matched 1-cm path length Suprasil quartz cells with Teflon stoppers. The copper cluster spectrum was generated by subtracting the spectrum of ACE1(122*) in the presence of 10 mM KCN, corrected for Cu(I)–$(CN)_x$ absorption, from that of Cu–ACE1(122*). Difference absorption spectra were resolved into component bands by deconvolution. As a component band shape, a Gaussian distribution as a function of wavenumber was assumed. The computer method used (NFIT; Island Products, Galveston, TX) was based on a nonlinear Marquardt–Levenberg fitting algorithm. The curve fitting was carried out at 1-nm intervals. The approximate spectral location of the component bands, entered as input values for the deconvolution routine, was determined from inspection of a second derivative spectrum.

Static luminescence measurements were carried out on a SLM 48000S spectrofluorometer as previously described (Casas-Finet et al., 1991), with emission spectra collected with a 10-mm Glan-Thompson polarizing filter inserted in the horizontal position in the emission path and a 450-nm low-pass filter in the excitation path. Excitation and emission monochromator slits were set at 1- and 8-nm bandwidths, respectively. Samples (200 μL) were held in a capped dual-path length (0.2 × 1.0 cm) Suprasil quartz cuvette in a thermostated cell holder, while the sample compartment was maintained under nitrogen atmosphere.

Dynamic luminescence experiments in the frequency domain were carried out at 25 °C with a Rhodamine 6G cavity-dumped dye laser, pumped by a mode-locked argon ion laser. The modulated excitation was obtained from the harmonic content of a laser pulse train with a repetition rate of 1.27 MHz and a pulse width of 5 ps. The emission was monitored with a microchannel plate photomultiplier tube with external cross-correlated detection. The frequency domain intensity data (phase and modulation) were fitted to a sum of exponential components by a nonlinear least-squares fit algorithm (Lakowicz, 1984). Cu–ACE1(122*) (7.0×10^{-5} M) and Ag–ACE1(122*) (1.5×10^{-4} M) samples were excited at 285 nm. A high-energy cutoff filter of 600 nm (Corning 3-71) was placed in the emission path.

Dynamic luminescence measurements in the time domain were carried out by the technique of time-correlated single-photon counting. Time-resolved fluorescence was measured on single-photon-counting instruments similar to those described by Badea and Brand (1979). Excitation was accomplished by the output of a PRA thyratron-gated nitrogen flash lamp. The excitation wavelength was 283 nm, and the emission wavelength was either 310 or 610 nm (8- or 16-nm bandwidth, respectively). Instrument response was corrected for wavelength-dependent transit time of the photomultiplier

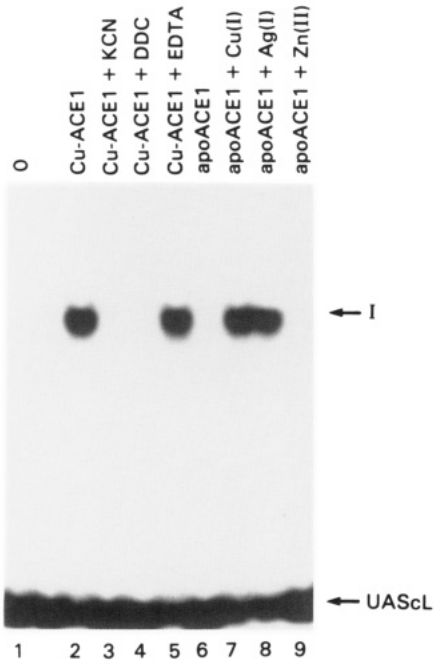

FIGURE 1: Metal binding analysis of ACE1(122*) peptide by gel retardation assays. In lanes 2–5, ACE1(122*) (0.1 μM) was incubated for 5 min with either KCN, diethyldithiocarbamate, or EDTA (2.0 μM) prior to the gel retardation assay. In lanes 6–9, apo-ACE1(122*) (0.5 μM) prepared by incubation of Cu–ACE1(122*) with 2 mM KCN followed by Sephadex G-50 chromatography in 5 mM potassium phosphate containing 50 mM KCl and 10 mM 2-mercaptoethanol was incubated with Cu(I)–acetonitrile, silver nitrate, or zinc sulfate (4.0 μM) for 30 min prior to the assay. Samples were assayed for binding to UAScL as described in Materials and Methods. The positions of the ACE1(122*)–UAScL complex and of the free UAScL oligonucleotide are indicated. Lane 1 contained no ACE1(122*) peptide.

tube. Data were analyzed by the procedure of Badea and Brand (1979).

Circular dichroism spectra were collected at 25.0 ± 0.1 °C on an AVIV 60DS CD spectrometer over the wavelength range 200–320 nm, using 0.2- or 1.0-cm path length Suprasil quartz cells, as described earlier (Casas-Finet et al., 1991). Theoretical CD spectra were generated using the parameters of Yang et al. (1986) and a computer-generated least-squares fit to the experimental data.

Results

Metal Binding and Reconstitution of ACE1(122).* As seen via gel mobility assays, binding of ACE1(122*) to the double-stranded oligonucleotide UAScL, carrying a high-affinity binding site, occurred only in the presence of Cu(I) or Ag(I) (Figure 1). No binding was observed when these metal ions were either absent or complexed by the monovalent ion chelators CN^- or diethyldithiocarbamate (DDC) (Figure 1). Zn(II) did not induce binding, nor did the divalent ion chelator EDTA inhibit the effect of Cu(I) or Ag(I) (Figure 1). Cu(I) or Ag(I) remained associated with the ACE1(122*) peptide, even in the presence of a high concentration of competing thiols used to maintain a reducing environment. A large excess of Ag(I) inhibited binding of ACE1(122*) to the UAScL oligonucleotide (Figure 2), probably due to the formation of Ag complexes with nonbridging sulfur thiolates, which bring about the destabilization of a functional cluster structure (Fürst & Hamer, 1989).

UV Spectroscopic Analysis of Cu–ACE1(122).* As previously reported (Casas-Finet et al., 1991), Cu–ACE1(122*) showed a broad optical transition in the ultraviolet which contains the overlapping contributions of the n → π^* tran-

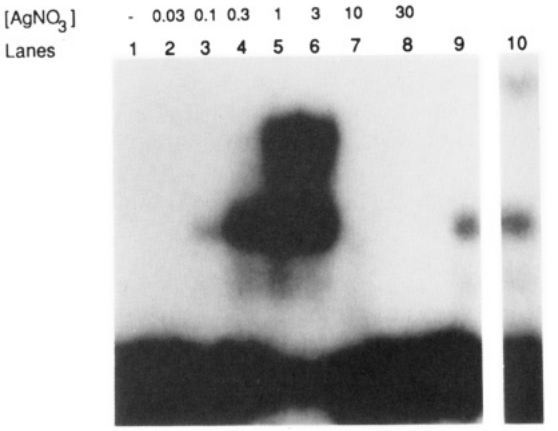

FIGURE 2: Ag reconstitution of ACE1(122*) in a crude *E. coli* extract monitored by band mobility shift assays with ^{32}P-labeled UASc oligonucleotide (lanes 2–8). Increasing amounts of $AgNO_3$ (0.1–30 mM final) were added to a Ag(I)-free extract. Notice the formation of a higher mobility complex in the [Ag(I)] range of 0.3–3 mM; half-site occupancy is seen at 0.1 and 10 mM $AgNO_3$. No binding was detected outside this range. Lane 1 contained no peptide; lanes 9 and 10 contained 0.2 and 0.4 mM $CuSO_4$ in the absence of Ag(I).

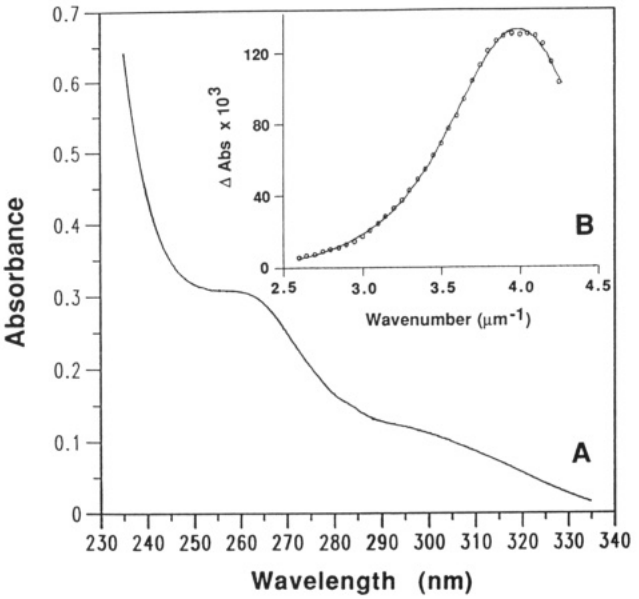

FIGURE 3: (A) UV absorption spectrum of the Cu(I) cluster of ACE1(122*) (65 μM) in 10 mM sodium phosphate, pH 6.15. (B) Fit of the Cu(I) cluster absorption (optical density vs wavenumber) to two Gaussian components, as described in Materials and Methods.

sitions of the peptidic amide bonds, the $\pi \rightarrow \pi^*$ transitions of Tyr-9 and Phe-55, and the electronic transitions of the copper center (Figure 3A). The contribution of the copper center disappeared upon acidification of ACE1(122*) to pH <1, which results in displacement of Cu(I) from the peptide by H^+ ions (Casas-Finet et al., 1991). A weak, broad copper transition, peaking in the 250–265-nm region, was obtained from the difference absorption spectrum (Casas-Finet et al., 1991). Its band shape and position, however, may be affected by the known pH dependence of tyrosine absorption, as changes in environmental polarity and hydrogen bonding can shift the absorption spectrum of tyrosine by as much as 4 nm (Lin & Liu, 1978; Strickland et al., 1972). The tyrosine spectrum of Cu(I)–metallothionein from *Neurospora* (Beltramini & Lerch, 1981) has been shown to be pH-dependent (Durell et al., 1990). Therefore, in this study the copper optical transitions were abolished by treatment of ACE1(122*) with the Cu(I) chelator CN^-. The difference spectrum displayed a peak at 232 nm, characteristic of a thiolate group, and a

distinct shoulder at 254 nm, assigned to the copper center absorption (not shown). This suggests the occurrence of ligand → Cu(I) charge-transfer electronic transitions with a bonding between Cu(I) and the cysteinyl thiolate of considerable covalent character; Cu(I) 3d → 4s Rydberg transitions are also possible (Tamilarasan & McMillin, 1986). Spectral deconvolution of the absorption spectrum (Figure 3B) showed that most of the absorbance of the copper center originated from an optical transition peaking at 249 ± 2 nm with a line width (fwhm) of 3600 cm^{-1}. This corresponds closely to the main band present in the excitation spectrum of the copper cluster luminescence of Cu–ACE1(122*) [see Figure 3 of Casas-Finet et al. (1991)]. A second, broader component of the cluster absorption spectrum, peaking at longer wavelengths, which is poorly constricted from spectral deconvolution is also apparent in the excitation spectrum of the cluster (Casas-Finet et al., 1991). Excitation at opposite edges of these overlapping optical transitions resulted in identical luminescence emission spectra (Casas-Finet et al., 1991), suggesting that they may consist of different excited-state configurations of a ligand-to-metal or intrametal electronic transition (see Discussion).

Ag–ACE1(122*) exhibited similar charge-transfer and/or metal-centered UV absorption bands which were abolished by CN^- or metal displacement by H^+ but not by the divalent ion chelator EDTA (not shown). The position of the optical transitions was shifted to higher energies, relative to those of the Cu complex, as Ag^+ has higher ionization energy than Cu^+ and ligand-to-metal charge-transfer energies depend upon the oxidizing character of the metal center (or, more precisely, on the combination of the redox potentials of the donor and acceptor atoms).

Steady-State Luminescence Spectroscopy. Both Cu(I)–ACE1(122*) (Casas-Finet et al., 1991) and Cu(I)–ACE1-(110*) (Figure 4A) exhibited a room-temperature orange luminescence (λ_{max} = 619 nm) typical of Cu–cysteinyl thiolate clusters. This luminescence emission was inhibited by the metal chelators KCN and DDC (Casas-Finet et al., 1991) or upon aerobic incubation, which is likely to lead to oxidation of the Cys residues.

Ag–ACE1(122*) exhibited a Tyr fluorescence spectrum with maximal emission intensity at 309 nm and a line width of 5000 cm^{-1}; the Tyr excitation spectrum peaked at 276 nm and was somewhat narrower (4600 cm^{-1}). A weak emission peaking at 605 nm was assigned to the luminescence originating from the Ag(I) metal cluster (Figure 4B); its integrated emission indicated a quantum yield of ca. 7% that of Cu-(I)–ACE1(122*). Contamination by a small amount of Cu-(I)–ACE1(122*) is unlikely, since both the wavelength of maximum emission of the Ag–ACE1(122*) sample and its line width (1600 cm^{-1}) differ from that of Cu(I)–ACE1(122*) [Casas-Finet et al. (1991); see also the Dynamic Luminescence Spectroscopy section]. The Ag(I)–ACE1(122*) luminescence excitation spectrum peaked at 272 nm (Figure 4C), which is in agreement with the wavelength of maximum absorbance for this system but not with the λ_{max} of the UV absorption or luminescence excitation spectra of Cu(I)–ACE1(122*) (Casas-Finet et al., 1991). Luminescence excitation or emission spectra collected for Ag(I)–ACE1(122*) in buffers containing 50% glycerol or 50% ethanol exhibited a small shift of their wavelength maxima of ~2 nm, indicating that the metal cluster has a rather weak exposure to the solvent.

Luminescence emission quenching of ca. 20% was seen upon binding Cu–ACE1(122*) to UAScL but not to either the scrambled sequence oligonucleotide MixL or double-stranded calf thymus DNA (Casas-Finet et al., 1991). Cu–ACE1-

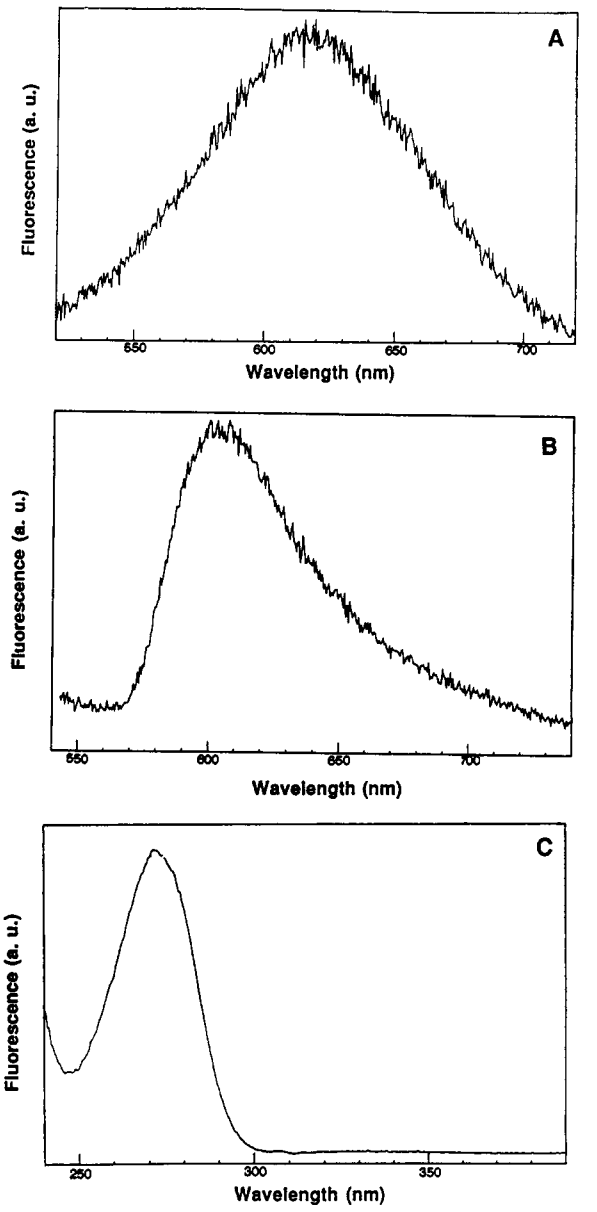

FIGURE 4: (A) Luminescence emission spectrum (uncorrected) of Cu–ACE1(110*) (10 μM) in 10 mM potassium phosphate, pH 6.15, at 25 °C. Excitation was at 250 nm (1-nm bandpass), and the emission monochromator was set at 8-nm resolution. (B) Luminescence emission spectrum (uncorrected) of Ag–ACE1(110*) (150 μM) in 10 mM potassium phosphate, pH 6.15, at 25 °C. Excitation was at 260 nm (2-nm bandpass), and the emission monochromator was set at 8-nm resolution. (C) Luminescence excitation spectrum (uncorrected) of Ag–ACE1(122*) (150 μM) in 10 mM sodium phosphate, pH 6.15, at 25 °C. Composite of two separate scans monitoring the emission at 585 and 640 nm (8-nm bandpass), normalized at 300 nm. Excitation monochromator was set at 1-nm resolution.

(110*) displayed luminescence quenching characteristics indistinguishable from those of the longer peptide (not shown). ACE1 peptides constitute, to our knowledge, the only reported case of a modulation of Cu(I)–thiolate luminescence by a ligand not interacting directly with the metal or sulfhydryl groups (Casas-Finet et al., 1991).

Tyr emission of Cu–ACE1(122*) was shown earlier to be quenched by approximately 30% by UAScL but not by double-stranded calf thymus DNA (Casas-Finet et al., 1991), indicating that the presence of the specific target sequence was necessary to induce such an effect. In agreement with this result, the oligonucleotide MixL also failed to induce Tyr quenching (not shown). Binding affinity was reduced upon increasing the ionic strength, suggesting the involvement of

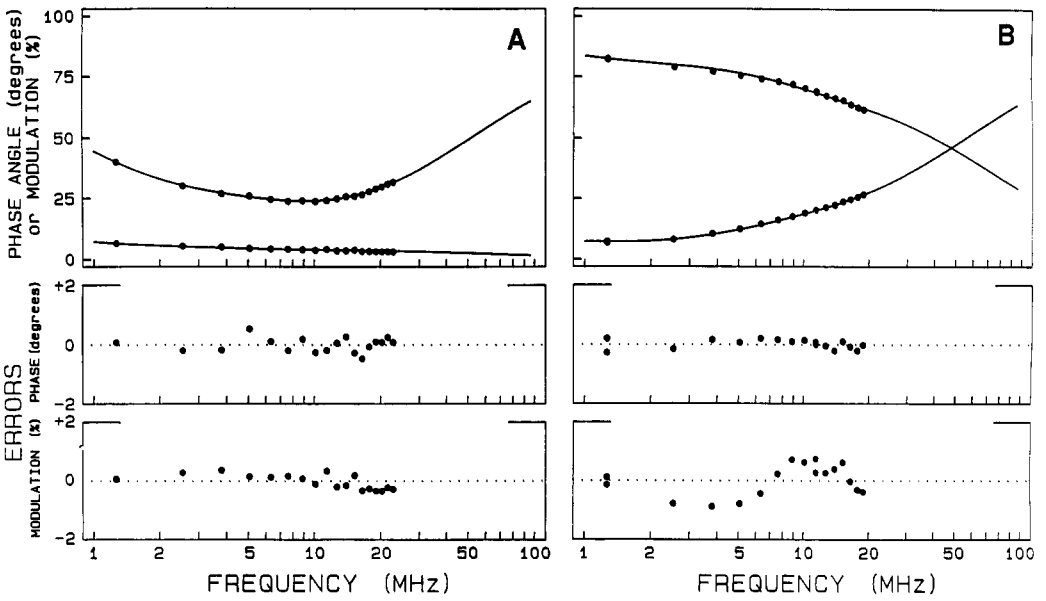

FIGURE 5: Frequency domain data for the intensity decay of metal cluster luminescence in (A) Cu–ACE1(122*) (70 μM) and (B) Ag–ACE1(122*) (150 μM). Continuous lines indicate a three-component fit through the data (decrease of modulation, increase of phase angle with increase of frequency).

basic residues from ACE1(122*). The UAScL, UAScM, UAScR oligonucleotides induced a quenching of ACE1(110*) Tyr fluorescence of a magnitude similar to that observed for Cu–ACE1(122*) in the presence of UAScL; the annealed oligonucleotide of sequence MixL was defective in the induction of such effect. Ag–ACE1(122*) also displayed a quenching of its Tyr emission in the presence of UAScL, but not MixL. In summary, these results indicate that, in the presence of Cu(I) or Ag(I), the N-terminal ACE-1 peptides were active in binding to the specific recognition sequence.

Dynamic Luminescence Spectroscopy. Dynamic luminescence measurements in the frequency domain of Cu–ACE1-(122*) (Figure 5A) and Ag–ACE1(122*) (Figure 5B) metal cluster emission were fitted to a sum of three exponential components (Figure 5A and B), which yielded randomly distributed residuals and reduced χ^2 values of ~1.0. A minor component of 3.40 (±0.03) ns, accounting for 3.7% of the steady-state emission intensity of Cu–ACE1(122*), was assigned to the average fluorescence lifetime of its single Tyr residue (see below), whose first Rayleigh harmonic at ca. 610 nm passes through the long-wave-pass filter in the emission path. Most of the luminescence of Cu–ACE1(122*), however, exhibited a lifetime of 3.2 (±0.1) μs (95% of the steady-state emission) with a minor component of 46 (±2) ns (1.4% of the steady-state emission). Disregarding the contribution of the Tyr fluorescence, the average luminescence lifetime of the Cu cluster in Cu–ACE1(122*) is, therefore, 3.2 μs. This relatively long lifetime at room temperature suggests that the luminescence originates from a spin-forbidden transition (phosphorescence).

Ag–ACE1(122*) also exhibited a contribution of its Tyr fluorescence, with a lifetime of 3.2 (±0.1) ns, to the metal cluster luminescence (Figure 5B). In this case it accounted, however, for 59% of the steady-state intensity above 600 nm. As the tyrosine fluorescence quantum yield and lifetimes of Ag– and Cu–ACE1(122*) are identical (see below), this indicates that the Ag cluster luminescence is much weaker (i.e., shorter lived) than that of the Cu cluster. This is shown by its luminescence lifetimes of 366 (±16) (20% of the steady-state intensity) and 18 (±1) ns (21% of the steady-state intensity). Disregarding the Tyr contribution, the average luminescence lifetime of the Ag cluster is 186 (±4) ns. This value is ca. 6% of that measured for Cu–ACE1(122*), in excellent agreement with the relative integrated luminescence emission of the cluster as determined in steady-state luminescence experiments (see above).

The Tyr fluorescence lifetime of Cu– and Ag–ACE1(122*) was measured by time-domain techniques and fitted to a sum of two exponential contributions (Figure 6A and B). The residuals of the fit were evenly distributed, and the lack of autocorrelation indicated their randomness; the reduced χ^2 of the fit was ~1.1. Cu–ACE1(122*) exhibited two lifetimes of 1.61 (±0.07) and 4.19 (±0.12) ns, with steady-state contributions of 46% and 53%, respectively. The Ag–ACE1(122*) Tyr fluorescence decay was fitted to two lifetimes of 1.70 (±0.03) and 4.29 (±0.02) ns, with steady-state contributions of 50% each. The average fluorescence lifetime of the Cu– and Ag–ACE1(122*) Tyr is 2.97 (±0.10) and 3.00 (±0.02) ns, respectively. The fluorescence decay properties of Tyr-7 in the Cu– and Ag–ACE1(122*) peptides are indistinguishable, indicating that its microenvironment is very similar, and suggesting that a direct interaction of the phenolic side chain with the metal cluster is unlikely (see Discussion).

Detector instability did not permit accurate determination of the long-lived cluster luminescence lifetime by time-domain techniques. However, a luminescence decay in the microsecond range was measured for Cu–ACE1(122*). No long-lived component was detected for Ag–ACE1(122*) (not shown), in agreement with the frequency domain measurements.

Circular Dichroism Spectroscopy. The CD spectra of Cu–ACE1(110*) exhibited a low content of long-range α-helical or β-sheet structure, as proposed earlier for the Cu–ACE1(122*) peptide (Casas-Finet et al., 1991; Dameron et al., 1991). The CD spectrum of Cu–ACE1(122*) could be best fit by a content of 14% α-helix, 17% β-structure, and 69% random coil (Figure 7). A reduction of ca. 20% in the magnitude of the negative ellipticity of Cu–ACE1(110*) was observed upon metal complexation by CN^- (not shown), indicating that the metal cluster stabilized the peptide's secondary structure. Ag–ACE1(122*) exhibited a CD spectrum similar to that of Cu–ACE1(122*), suggesting that both ions induced a similar folded structure. Ag(I) binding stabilized ACE1(122*) against GuHCl denaturation, relative to the apoprotein form, as indicated by the reduced effect of dena-

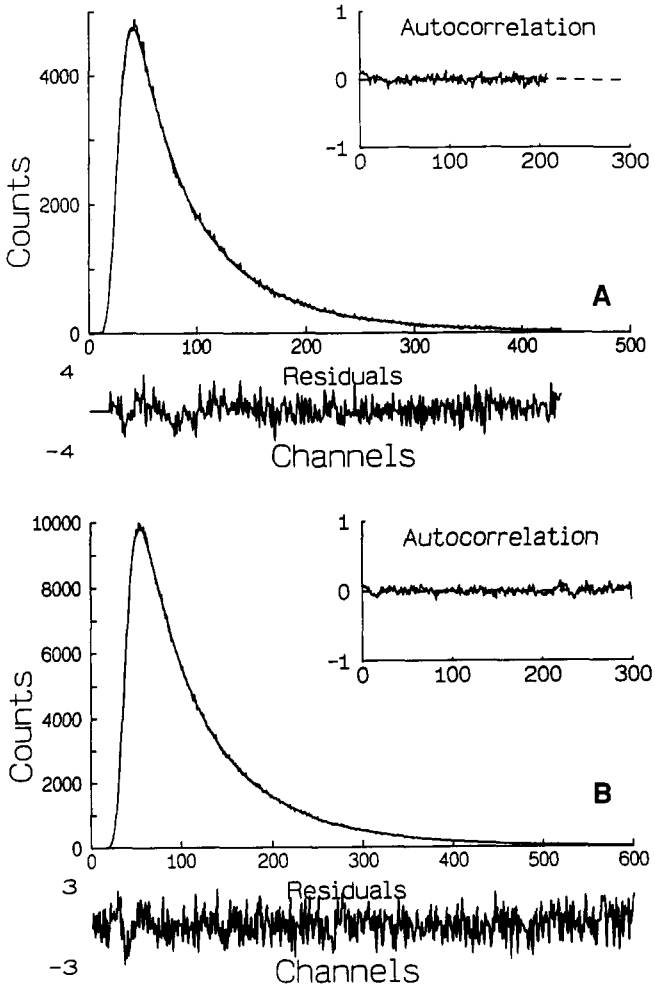

FIGURE 6: Fluorescence decay of Tyr in (A) Cu–ACE1(122*) (70 μM) and (B) Ag–ACE1(122*) (150 μM) following pulse excitation. Continuous lines indicate a three-component fit (two lifetimes plus background) through the data. About 1.4×10^5 total counts were accumulated and analyzed. Residuals of the fit (in percentage units) and autocorrelation plot are shown in inset.

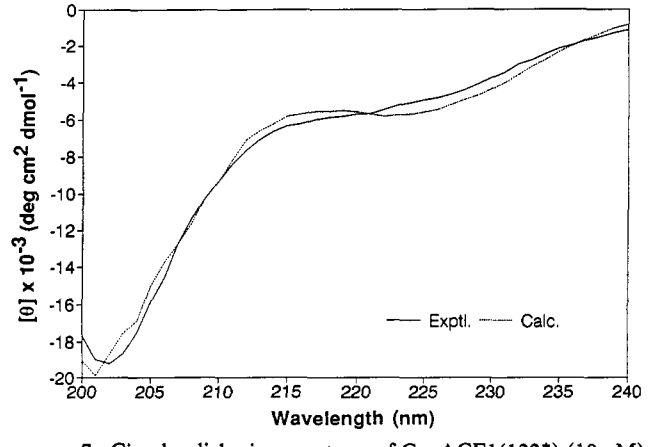

FIGURE 7: Circular dichroism spectrum of Cu–ACE1(122*) (10 μM) in 5 mM sodium phosphate, pH 6.15, at 25 °C. Five spectra were recorded, averaged, corrected for background, and smoothed (solid line). Secondary structure prediction was carried out by computer fitting against a parametric data set according to Yang et al. (1986), as described in Materials and Methods.

turant agent on protein ellipticity in the presence of metal (not shown).

Discussion

Specificity of Metal and DNA Binding. The metal-binding specificity of the ACE1(122*) peptide (Figure 1) is in agreement with previous results obtained for the intact protein indicating that only Cu(I) and Ag(I) [but not Zn(II), Pb(II), Cd(II), or Ni(II)] are able to induce binding of ACE1 to the UAScL oligonucleotide (Fürst et al., 1988) or to stimulate transcription in vitro (Culotta et al., 1989). The monovalent ion chelators KCN and diethyldithiocarbamate (DDC) completely inhibited both the binding of ACE1 to UAScL (Fürst et al., 1988) and the onset of ACE1-mediated transcription (Culotta et al., 1989). In contrast, the divalent metal chelator EDTA did not prevent Cu(I) binding to ACE1(122*), nor was the formation of a UAScL–ACE1(122*) complex induced by Zn(II). High concentrations of either Ag(I) (Figure 2) or Cu(I) (Fürst & Hamer, 1989) result in destabilization or oxidation of the metal–thiolate cluster, as observed for Cu(I)–metallothionein (Byrd et al., 1988). This result is also in agreement with Cu(I) reconstitution experiments carried out monitoring the ACE1(122*) metal cluster luminescence (Dameron et al., 1991), in which addition of excess Cu(I) above the stoichiometric amount induced a decrease of the emission intensity from its maximal value. The sensitivity of the DNA binding activity of ACE1 to the monovalent metal ion concentration may account for its function as a regulatory element; at least in part, the rapid drop in activity at higher metal concentrations may contribute to the observed cell toxicity under such conditions.

Band shift assays show that Ag(I) binding to ACE1(122*) is characterized by a lower threshold but proceeds in a less cooperative fashion than that of Cu(I) (Fürst & Hamer, 1989). Band shift assays of Ag(I)–ACE1(122*) are clearly biphasic (Figure 2), leveling off at intermediate metal concentrations and requiring rather high [Ag^+] for maximum binding [see Figure 2 of Fürst and Hamer (1989)] and formation of a higher mobility complex. Note that addition of Ag(I) induces a mobility shift of both the lower mobility complex, which is known to result from binding of the ACE1(122*) peptide to the leftward site of the UASc oligonucleotide, and the higher mobility complex corresponding to the occupancy of both sites (Hu et al., 1990). This suggests that binding to the tandem sites of UASc occurs in an independent manner.

Binding of Cu–ACE1(122*) to various oligonucleotides spanning overlapping sections of the specific recognition site UASc suggests that contacts with the DNA-binding domain occur with both the outermost part of the 5′ and 3′ half-sites and the central region of the UASc site spanning the pseudodyad symmetry axis, in agreement with a recent study of hydroxyl radical cleavage and methylation interference (Buchman et al., 1990).

Absorption Spectra. Characteristic near-UV optical transitions of the metal center are abolished upon metal chelation or displacement at low pH. Removal of Cu(I) from ACE1(122*) by complexation with CN^-, unlike displacement by H^+, prevents possible pH effects on tyrosine absorption and is likely to yield an unperturbed aromatic absorption spectrum in apo-ACE1(122*), relative to Cu–ACE1(122*), on the assumption that the aromatic $\pi \rightarrow \pi^*$ transitions are not strongly coupled to those of the copper center (in which case an exchange of oscillator strength between them could be possible). Such coupling seems unlikely, given that the paucity of aromatic residues in this class of proteins is thought to result from the unfavorable environment about the metal cluster for such hydrophobic amino acids.

Although it is not possible at present to identify with certainty the electronic transitions which cause the optical properties of the copper center, a plausible assignment would

include charge-transfer or metal-centered transitions. Transitions essentially localized on the metal (m → m*) appear unlikely since, in the absence of significant interaction with the ligand orbitals, the luminescence emission would exhibit a sharp line spectrum without any appreciable structure (Lyttle, 1970). Transitions purely localized on the ligand (l → l*) are not consistent with the observation of a metal absorption band to the red of the long-wavelength ligand band (Lyttle, 1970). Transitions involving both manifolds (charge transfer) are supported by the appearance of a new absorption band, the absence of pure ligand or metal optical transitions at lower energies than the long-wavelength charge-transfer band, and by the fact that ions forming these complexes are usually easy to oxidize and must be diamagnetic (Lyttle, 1970). A theoretical treatment of a $[Cu_8S_{12}]^{4-}$ cluster (Fackler, 1976) suggests that the highest filled molecular orbitals of the cluster have some metal character but are predominantly sulfur 3p; the lowest empty molecular orbitals are primarily copper 4s and 4p. This would lead to the prediction of l → m* transitions. The electronic transitions in the Cu(I) cluster of ACE1(122*) could be of similar origin, originating from ligand → metal charge-transfer transitions. More specifically, the two Guassian transitions that fit the copper cluster absorption spectrum (Figure 3B) could be assigned to S(Cys) → Cu(I) components originating from distinct lone pairs of the cysteine sulfur. Intrametal 3d → 4s Rydberg transitions have also been proposed for Cu(I) complexes (Payne et al., 1984). In either case, the transitions involve a radial displacement of electron density away from the 3d shell of the Cu(I) center. An analogous assignment is possible for the Ag(I) complex, although given that an isomorphous Ag center might be less compact and more solvent-exposed, charge-transfer-to-solvent transitions may be present as well (Tamilarasan & McMillin, 1986); these have been proposed also to occur in the near-UV spectra of Cu(I) complexes (David et al., 1978).

Luminescence Spectra. The Tyr fluorescence emission spectra and lifetimes of Cu(I)- and Ag(I)-ACE1(122*) are virtually identical, suggesting that the microenvironment of this residue is comparable in either complex. The long luminescence lifetime of Cu-ACE1(122*), together with its very large Stokes shift and the quenching of its emission intensity by molecular oxygen (Casas-Finet et al., 1991), suggests that the emission originates from a triplet state. Different excited states may arise, depending on which of the split metal 3d orbitals is the origin of the promoted electron; although the 3d orbitals of copper in a $[Cu_8S_{12}]^{4-}$ cluster are not predicted to be split significantly (Fackler, 1976), the levels can differ in spin multiplicity (Blasse & McMillin, 1980). In fact, given that intersystem crossing is usually rapid in metal complexes (Porter, 1975), the lowest energy excited state is expected to be a triplet state. Luminescence lifetime measurements of Cu(I)-metallothionein at 298 K show a component of 3.5 μs, which has been assigned to a metal-centered transition $^3[3d^9 4s^1] \rightarrow {}^1[3d^{10}]$ (Gasyna et al., 1988). This intra-copper(I) transition is orbitally forbidden and is expected to have a lifetime in the microsecond range. The predominant 3.2-μs component in the Cu(I)-ACE1(122*) luminescence may have a similar orbital parentage. The relatively fast 46-ns component observed in the luminescence emission of Cu-ACE1(122*) could be the emission from a singlet excited state associated with this interconfiguration transition (Payne et al., 1986).

The luminescence emission of Ag-ACE1(122*) is weaker and blue-shifted relative to that of Cu-ACE1(122*), in agreement with results obtained from studies of Ag(I) and Cu(I) mercaptides in the solid state (Anglin et al., 1971). The cluster luminescence emission of Ag-ACE1(122*) is predicted to be very weak in fluid samples, as all previous reports of luminescence from Ag(I) complexes have been documented for solids or frozen samples at cryogenic temperature. Although one cannot completely exclude the possibility that the room-temperature luminescence emission of Ag-ACE1(122*) reported in this study could originate from a small amount of contaminanting Cu-ACE1(122*), the copper content of the purified Ag-ACE1(122*) peptide was measured to be less than 2% of the stoichiometric amount. Since the integrated luminescence emission of Ag-ACE1(122*), on the other hand, is ~7% of that observed for Cu-ACE1(122*), mere contamination by Cu(I)-bound peptide could not account for the observed emission. Interestingly, the average luminescence lifetime of Ag-ACE1(122*) is ca. 6% of that of Cu-ACE1(122*). As Ag-ACE1(122*) has luminescence lifetime components very different from those of Cu-ACE1(122*), we believe that the emission indeed originates from the Ag cluster. If so, the weak luminescence emission detected for Ag-ACE1(122*) is the first reported room-temperature emission in a solution of a luminescent complex of silver.

ACE1 Secondary Structure. The unusual CD spectrum of Cu- or Ag-ACE1(122*) was expected from 2D-NMR studies with rabbit liver metallothionein, which indicated a 3_{10}-helical structure, rather than the more common α-helices, together with numerous inverted type II tight turns which appear to be a consequence of the structural constraints imposed on the polypeptide conformation by the large number of metal-binding sites (Wagner et al., 1986). That this constrained structure is particularly favorable for specific DNA binding is proven by the fact that in the presence of UASc oligonucleotide the affinity of Ag(I) for ACE1 is much higher than in its absence (Fürst and Hamer, 1989).

It has been proposed that wrapping of ACE1 around the Cu(I)-S scaffold of the cluster leads to the formation of positively charged loop structures which bind DNA specifically (Hu et al., 1990). The arrangement of 10 of the 12 cysteine residues as Cys-X-Cys or Cys-X-X-Cys pairs found in ACE1 and metallothionein has been proposed to induce a favorable geometry for metal coordination by the sulfur atoms (Frey et al., 1985), resulting in characteristic tight-turn structures for the short loops between the two cysteines (Wagner et al., 1986). Model building suggests that the two cysteine thiolates in one such pair can bind to Cu(I) in two contiguous edges of a proposed cuboidal cluster (Fürst et al., 1988). The two unpaired cysteine residues, located in the proximal and distal region of the cluster's primary sequence (Fürst et al., 1988), may be brought together to close the cluster structure, further suggesting that metal complexation results in the formation of a very tight, extremely compact structure. It is known that the apoprotein forms of metallothionein (Winge et al., 1985), ACE1 (Fürst et al., 1988), ACE1(122*) (Fürst & Hamer, 1989), and ACE1(110*) (Hu et al., 1990) are highly susceptible to a variety of proteases, whereas the metalloprotein forms are completely resistant. Ag(I) is a good electronic analog of Cu(I) and has been shown to bind to metallothionein with the same stoichiometry and coordination properties as copper (Winge et al., 1985). While Ag(I) binds ACE1(122*) and activates DNA binding and transcription, suggesting that it is capable of forming a metal cluster structurally similar to that of Cu(I), the larger ionic radius of Ag may be responsible for the lower stability of the metal complex and the smaller size of the protected peptide in proteolysis assays (Fürst & Hamer, 1989). Studies of model compounds show an av-

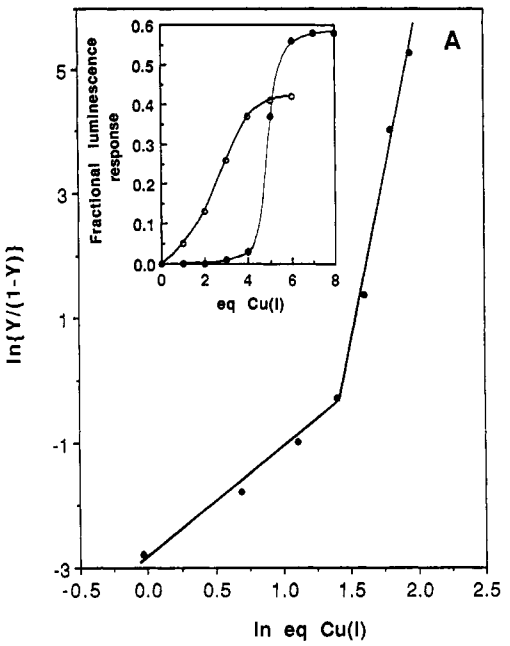

FIGURE 8: (A) Hill plot of the Cu(I) reconstitution data presented in Figure 2B of Dameron et al. (1991). (B) Inset: deconvolution of the sigmoidal luminescence recovery curve of ACE1(122*) in the presence of 0–8 mol equiv of Cu(I) to two symmetric sigmoidal components.

erage bond distance of 2.502 Å for trigonal Ag(I)–S compared with 2.270 Å for Cu(I)–S (Dance, 1978). The larger metal cluster in Ag–ACE1(122*) may also provide a poorer shielding from solvent, relative to the more compact copper cluster. This may result in a more efficient quenching of the metal cluster luminescence through a collisional process with solvent molecules. It is worth noting that, for poorly shielded inorganic Cu(I) complexes with thiol ligands, luminescence emission has been only observed in dried samples (Anglin et al., 1971) or in disordered (glassy) samples at 77 K (Buchner & McMillin, 1978).

Stoichiometry of the Metal Cluster. The dependence of the luminescence emission intensity on the chelation state of the peptide and degree of solvent shielding is supported by Cu(I) reconstitution studies of metal-depleted ACE1(122*), showing a sigmoidal luminescence recovery curve upon addition of succesive equivalents of Cu(I) (Dameron et al., 1991). Luminescence emission intensity was maximal at a copper-to-peptide stoichiometry of 7–8; further addition of Cu(I) resulted in a luminescence decrease, suggesting that this is the optimum stoichiometry for the induction of an ordered metal cluster structure (Dameron et al., 1991). We found that a Hill plot of this S-shaped curve gave a weighted Hill coefficient of 6 (Figure 8); the Hill coefficient for the binding of n molecules of ligand to a substrate can vary from a minimum of 1 for completely noncooperative binding to a maximum of n for a infinitely cooperative interaction between the binding sites. These results indicate that 6 is the minimal Cu(I) stoichiometry of the ACE1(122*) peptide, and that binding of copper is a highly cooperative process, with initial Cu(I) binding strongly stimulating additional metal uptake. A consequence of this strong cooperativity is that, at subsaturating concentrations of metal, most of ACE1 will be in two distinct populations: metal-free and fully Cu-saturated. It has been pointed out that the cooperative interaction between Cu and ACE1 may be necessary for a large cell response in gene expression to a small change in effector metal concentration (Fürst & Hamer, 1989). Previous band mobility shift assays indicated a high cooperativity of copper binding to ACE1(122*), with a Hill coefficient of 4.2 (Fürst & Hamer, 1989). A direct comparison of this value with that obtained from the luminescence recovery curve is not straightforward, however, since the band mobility shift assay monitored binding activity of ACE1(122*) to the specific high-affinity substrate UASc. On the other hand, even at intermediate metal occupancy, solvent extrusion from the metal cluster (not necessarily of the same structure as that of the cluster formed in the active peptide at optimal stoichiometry) can result in luminescence emission whose yield may depend on the Cu(I) ligand field (Thrower et al., 1988).

From the maximum values (Dameron et al., 1991) for the stoichiometry of native isolates of Cu–ACE1(122*) (8 mol/mol of peptide) and Ag–ACE1(122*) (9 mol/mol of peptide) and the saturation values obtained in Cu(I) reconstitution experiments of apo-ACE1(122*) monitoring metal cluster absorbance (6 mol/mol of peptide) or luminescence (7 mol/mol of peptide) (Dameron et al., 1991), the true stoichiometry seems to be around 7–8. It is worth noting that a Hill plot analysis of published luminescence recovery curves [Figure 2B of Dameron et al. (1991)] shows a clear biphasic behavior, with a first step of moderate cooperativity followed by a second, much more cooperative step (Figure 8A). The discontinuity in the plot occurs at 4 mol of Cu/mol of peptide (Figure 8A). Since the luminescence quantum yield may not exhibit a linear dependence with the fractional metal occupancy, we fitted the data to a linear combination of two symmetric sigmoidal curves with floating limiting quantum yields. The best fit consisted of a first component that accounts for 42% of the final emission intensity and that is ~90% complete at a stoichiometry of 4; the second component accounts for 58% of the final emission intensity of the cluster and is only 5% populated at a stoichiometry of 4 (Figure 8B). This second component increases steeply with increasing molar equivalents of Cu(I) and accounts for an additional 3–4 mol/mol of peptide (Figure 8B). This suggests that ACE1 may contain two distinct clusters. Note that ACE1(122*) with intermediate Cu(I) stoichiometries of 4 have been both isolated from an heterologous expression system and reconstituted in vitro (Dameron et al., 1991).

Structure of the Metal Cluster. In a recent study, Dameron et al. (1991) showed, using X-ray absorption spectroscopy, that Cu–ACE1(122*) contains a polynuclear Cu(I)–S cluster in which Cu(I) is triply coordinated to sulfur in a distorted trigonal coordination environment with average Cu–S and Cu···Cu distances of 2.26 (±0.02) and 2.68 (±0.04) Å, respectively. A similar environment has been described for Cu–metallothionein (George et al., 1988), characterized by a Cu–S distance of 2.23 Å and two types of Cu···Cu distances of 2.67 and 3.93 Å. A model has been proposed for Cu–metallothionein (George et al., 1988) and Cu–ACE1(122*) (Fürst et al., 1988) in which a copper atom occupies each corner of a flattened cube with (Cu···Cu) edge distances of 2.67, 2.67, and 3.9 Å, and cysteine sulfur ligand bridges over each of the 12 edges (note the Cu_8Cys_{12} stoichiometry of Cu–metallothionein). However, for inorganic Cu(I) clusters, reported Cu···Cu distances range from 2.38 (Guss et al., 1972) to 3.45 Å (Churchill & Kalra, 1974) with numerous other Cu(I) cluster compounds with intermediate values between these two extremes. A distance of 3.9 Å would be clearly outside this range; it was solely attributed to a Cu···Cu edge distance in the single-cluster Cu_8Cys_{12} model since, in general, long-distance interactions between pairs of copper atoms which are not directly bridged by a sulfur would be expected to be

damped out by thermal or static disorder (George et al., 1988). We propose that this model is incorrect and suggest an alternative model in agreement with the results in the literature for cubic octanuclear Cu(I) clusters.

Note that electronic shell closure requirements are not satisfied for a Cu_8S_{12} cluster: assuming that each Cu(I) contributes 10 electrons and each sulfur atom 4 electrons to the bonding in the octanuclear Cu(I) cluster, the system is 16 electrons short of achieving a closed-shell noble gas configuration, or 2 electrons per copper atom. In order to give each copper atom the favored 18-electron configuration, the copper cube must contain eight copper–copper bonds, suggesting a valence-bond description with a fractional bond order of 2/3. Although molecular orbital calculations based on atomic functions of the 8 copper and 12 sulfur atoms and idealized O_h (cubic) symmetry suggested that the Cu–Cu interaction was on the whole slightly repulsive rather than attractive (Hollander & Coucouvanis, 1974; Fackler, 1976), the observed constancy of the copper–copper distance in octanuclear Cu(I) bound to sulfur ligands with large differences in their S···S "bite" distance strongly suggests that there is an attractive, albeit perhaps weak, interaction (bonding) between the copper atoms of the cube (Hollander & Coucouvanis, 1974). One would predict, therefore, that the copper atoms would be at equal distance from each other, with the Cu_8S_{12} core of the cluster assuming T_h symmetry. This would suggest that the outer shell EXAFS data for Cu–metallothionein, indicating backscattering copper atoms at 3.9 Å (George et al., 1988), could originate from Cu(I) facing opposite corners of the cubic faces of the cluster (Cu···Cu distance 3.8 Å). The unusual rigidity of the Cu_8S_{12} cluster, in which a cube of copper atoms is embedded within an icosahedron defined by the 12 sulfur atoms of the ligands, with each copper coordinated by three sulfur atoms from different ligands and each sulfur bridging two copper atoms on an edge of the cube, may account for the detection of this outer shell backscattering contribution to the Cu K-edge EXAFS Fourier transform of Cu–metallothionein. It is worth noting that in Cu–metallothionein mutants lacking two and four cysteine sulfurs (but containing about seven copper atoms per molecule), for which it has been suggested that a corner or edge of the octanuclear cubic cluster would be missing (George et al., 1988), the Cu···Cu absorber–scatterer signal at 3.9 Å could not be distinguished from the noise (George et al., 1988). Note that a recent NMR study on yeast metallothionein, using Ag(I) as an isomorphic replacement for copper (Narula et al., 1991), showed that only thiolate groups, but no histidyl side chain, were involved in metal chelation. Bound Ag(I) originated seven distinct resonances with connectivities to 10 of the 12 cysteines (Narula et al., 1991).

Since EXAFS data for reconstituted Cu_4–ACE1(122*) and $Cu_{6.8}$–ACE1(122*) samples are very similar (Dameron et al., 1991), it is conceivable that ACE1 could possess two identical clusters which could be involved in the binding to the two half-sites of the recognition sequence. It is worth noting that mutation of a single Cys results in a variant protein that interacts with only one part of the wild-type site (Buchman et al., 1990). Another possibility is that the cuboidal cluster can be built in two steps, perhaps by apposition of two planar square clusters of four Cu atoms each constituting opposite faces in the cubic structure or by expansion of a tetrahedron inscribed within the cube. Although the X-ray absorption data generated by these intermediate structures would be expected to differ from that of the native ACE1 species, the high cooperativity of the putative second step of metal uptake proposed from our analysis of reconstitution studies could result in a significant population of only the fully metalated and apopeptide states. The experimental data so far available are in agreement with an octanuclear Cu(I) or Ag(I) μ-thiolate structure adopting cubic symmetry; however, the precise stoichiometry and structure of the polynuclear metal cluster of ACE1 is not yet clear. Further studies will be needed to elucidate the structure of these metal clusters.

Acknowledgments

We are grateful to Drs. Henryk Malak and Joseph Lakowicz (Center for Fluorescence Spectroscopy, University of Maryland at Baltimore) and Peng-Guang Wu and Ludwig Brand (Johns Hopkins University) for their assistance with the dynamic fluorescence measurements. We thank Drs. Enrico Bucci and Clara Fronticelli (University of Maryland at Baltimore) for access to the CD spectrometer and their helpful assistance.

References

Anglin, J. H., Batten, W. H., Jr., Raz, A. I., & Sayre, R. M. (1971) *Photochem. Photobiol. 13*, 279–281.

Badea, M. G. & Brand, L. (1979) *Methods Enzymol. 61H*, 378–394.

Beltramini, M., & Lerch, K. (1981) *FEBS Lett. 127*, 201–203.

Blasse, G., & Mc Millin, D. R. (1980) *Chem. Phys. Lett. 70*, 1–3.

Buchman, C., Skroch, P., Dixon, W., Tullius, T. D., & Karin, M. (1990) *Mol. Cell. Biol. 10*, 4778–4787.

Buchner, M. T., & Mc Millin, D. R. (1978) *J. Chem. Soc., Chem. Commun.* 759.

Byrd, J., Berger, R. M. McMillin, D. R., Wright, C. F., Hamer, D., & Winge, D. R. (1988) *J. Biol. Chem. 263*, 6688–6694.

Casas-Finet, J. R., Hu, S., Hamer, D., & Karpel, R. L. (1991) *FEBS Lett. 281*, 205–208.

Casas-Finet, J. R., Fischer, K. R., & Karpel, R. L. (1992) *Proc. Natl. Acad. Sci. U.S.A. 89*, 1050–1054.

Churchill, M. R., & Kalra, K. L. (1973) *J. Am. Chem. Soc. 95*, 5772–5773.

Culotta, V. C., Hsu, T., Hu, S., Fürst, P., & Hamer, D. (1989) *Proc. Natl. Acad. Sci. U.S.A. 86*, 8377–8381.

Dameron, C. T., Winge, D. R., George, G. N., Sansone, M., Hu, S., & Hamer, D. (1991) *Proc. Natl. Acad. Sci. U.S.A. 88*, 6127–6131.

Dance, I. G. (1978) *Aust. J. Chem. 31*, 2195–2206.

David, D. D., Stevenson, K. L., & Davis, C. R. (1978) *J. Am. Chem. Soc. 100*, 5344–5349.

Durell, S. R., Lee, C.-H., Ross, R. T., & Gross, E. L. (1990) *Arch. Biochem. Biophys. 278*, 148–160.

Fackler, J. P., Jr. (1976) in *Progress in Inorganic Chemistry* (Lippard, S. J., Ed.) pp 55–103, John Wiley and Sons, New York.

Frey, M. H., Wagner, G., Vasák, M., Sørensen, O. W., Neuhaus, D., Wörgötter, E., Kägi, J. H. R., Ernst, R. D., & Wüthrich, K. (1985) *J. Am. Chem. Soc. 107*, 6847–6851.

Fürst, P., & Hamer, D. (1989) *Proc. Natl. Acad. Sci. U.S.A. 86*, 5267–5271.

Fürst, P., Hu, S., Hackett, R., & Hamer, D. (1988) *Cell 55*, 705–717.

Gasyna, Z., Zelazowski, A., Green, A. R., Ough, E., & Stillman, M. J. (1988) *Inorg. Chim. Acta 153*, 115–118.

George, G. N., Byrd, J., & Winge, D. R. (1988) *J. Biol. Chem. 263*, 8199–8203.

Guss, J. M., Mason, R., Sotofte, I., van Koten, G., & Noltes, J. G. (1972) *J. Chem. Soc., Chem. Commun.* 446.

Hemmerich, P., & Sigwart, C. (1963) *Experientia 19*, 488–489.
Hollander, F. G., & Coucouvanis, D. (1974) *J. Am. Chem. Soc. 96*, 5646–5648.
Hu, S., Fürst, P., & Hamer, D. (1990) *New Biol. 2*, 544–555.
Lakowicz, J. R., Laczko, G., Cherek, H., Gratton, E., & Limkeman, M. (1984) *Biophys. J. 46*, 463–477.
Lin, C.-H., & Liu, S.-H. (1978) *J. Chin. Chem. Soc. 25*, 167–177.
Lyttle, F. E. (1970) *Appl. Spectrosc. 24*, 319–326.
Narula, S. S., Mehra, R. K., Winge, D. R., & Armitage, I. M. (1991) *J. Am. Chem. Soc. 113*, 9354–9358.
Payne, S. A., Goldberg, A. B., & Mc Clure, D. S. (1984) *J. Chem. Phys. 81*, 1529–1537.
Payne, S. A., Chase, L. L., & Boatner, L. A. (1986) *J. Lumin. 35*, 171–177.
Porter, G. B. (1975) in *Concepts of Inorganic Photochemistry* (Adamson, A., & Fleischauer, P. D., Eds.) Chapter 2, Wiley Interscience, New York.
Strickland, E. H., Wilchek, M., Horwitz, J., & Billups, C. (1972) *J. Biol. Chem. 247*, 572–580.
Tamilarasan, R., & McMillin, D. R. (1986) *Inorg. Chem. 25*, 2037–2040.
Thiele, D. J. (1988) *Mol. Cell. Biol. 8*, 2745–2752.
Thrower, A. R., Byrd, J., Tarbet, E. B., Mehra, R. K., Hamer, D. H., & Winge, D. R. (1988) *J. Biol. Chem. 263*, 7037–7042.
Yang, J. T., Wu, C.-S. C., & Martinez, H. M. (1986) *Methods Enzymol. 130*, 208–269.
Wagner, G., Neuhaus, D., Wörgötter, E., Vasák, M., Kägi, J. H. R., & Wüthrich, K. (1986) *J. Mol. Biol. 187*, 131–135.

CORRECTION

A Scanning Calorimetric Study of the Thermal Denaturation of the Lysozyme of Phage T4 and the Arg 96 → His Mutant Form Thereof, by Shinichi Kitamura and Julian M. Sturtevant*, Volume 28, Number 9, May 2, 1989, pages 3788–3792.

Page 3791. Equation A4 should read

$$\Delta h_o = \Delta h_{1/2} - (C - A)t_{1/2} - (1/2)(D - B)t_{1/2}^2 \quad \text{(A4)}$$

Page 3792. Equation A8 should read

$$c_{ex} = \Delta h_{cal}\frac{d\alpha}{dT} = \alpha(1 - \alpha)\frac{\beta\Delta h_{cal}}{RT^2} \quad \text{(A8)}$$